NSRRC-J05072(2016)

LANGMUIR

Article

pubs.acs.org/Langmuir

Small-Angle Neutron Scattering Studies on the Multilamellae Formed by Mixing Lamella-Forming Cationic Diblock Copolymers with Lipids and Their Interaction with DNA

Po-Wei Yang,[†] Tsang-Lang Lin,[*,†] I-Ting Liu,[†] Yuan Hu,[†] U-Ser Jeng,[‡] and Elliot Paul Gilbert[§]

[†]Department of Engineering and System Science, National Tsing Hua University, Hsinchu 300, Taiwan, Republic of China

[‡]National Synchrotron Radiation Research Center (NSRRC), Hsinchu, 300, Taiwan, Republic of China

[§]Bragg Institute, Australian Nuclear Science and Technology Organisation (ANSTO), Locked Bag 2001, Kirrawee DC, New South Wales 2232, Australia

Supporting Information

ABSTRACT: We demonstrate that the lamella-forming polystyrene-*block*-poly(*N*-methyl-4-vinylpyridinium iodine) (PS-*b*-P4VPQ), with similar sizes of the PS and P4VPQ blocks, can be dispersed in the aqueous solutions by forming lipid/PS-*b*-P4VPQ multilamellae. Using small-angle neutron scattering (SANS) and 1,2-dipalmitoyl-d_{62}-*sn*-glycero-3-phosphocholine (d_{62}-DPPC) in D_2O, a broad correlation peak is found in the scattering profile that signifies the formation of the loosely ordered d_{62}-DPPC/PS-*b*-P4VPQ multilamellae. The thicknesses of the hydrophobic and hydrophilic layers of the d_{62}-DPPC/PS-*b*-P4VPQ multilamellae are close to the PS layer and the condensed brush layer thicknesses as determined from previous neutron reflectometry studies on the PS-*b*-P4VPQ monolayer at the air–water interface. Such well-dispersed d_{62}-DPPC/PS-*b*-P4VPQ multilamellae are capable of forming multilamellae with DNA in aqueous solution. It is found that the encapsulation of DNA in the hydrophilic layer of the d_{62}-DPPC/PS-*b*-P4VPQ multilamellae slightly increases the thickness of the hydrophilic layer. Adding $CaCl_2$ can enhance the DNA adsorption in the hydrophilic brush layer, and it is similar to that observed in the neutron reflectometry study of the DNA adsorption by the PS-*b*-P4VPQ monolayer.

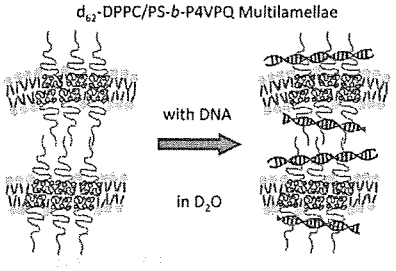

INTRODUCTION

Recently, there have been intensive studies on lipid–DNA multilamellae as a result of the need to develop high-efficiency gene delivery systems for non-viral gene therapy.[1−7] Previously, we studied the interaction of DNA with cationic cholesterol monolayers at the air–liquid interface by neutron reflectivity,[8] and also in solution by small-angle X-ray scattering (SAXS).[9] These studies showed that DNA can be effectively adsorbed to the cationic lipid monolayer or bilayer surfaces. As revealed by X-ray or neutron scattering studies, well-ordered lipid–DNA multilamellae can be successfully formulated by carefully tuning the surface charge density and the mixture of cationic lipids with neutral or helper lipids. Although using cationic lipids is quite successful in encapsulating the DNA, it is still desirable to develop alternatives, such as using cationic diblock copolymers, which have the advantage of possessing cationic brushes that could form three-dimensional structures with DNA.[10] Amphiphilic diblock copolymers can form highly stable vesicles or micelles in solutions, which can be used to form multilamellae with DNA through charge interactions.[11,12] DNA interacts strongly with the cationic blocks to form highly stable polyplexes as a result of the entropic gain of releasing the small ions from the DNA and the cationic brush. Using a diblock copolymer system, it is possible to enhance the adsorption of DNA with the charged brushes, as compared to planar lipid bilayers. A study using neutron reflectometry from a diblock copolymer monolayer at the air–water interface with DNA in the subphase indicated that high amounts of DNA could be adsorbed in the cationic brush layer.[10] However, such diblock copolymers that can form a stable planar structure (having a comparable hydrophilic block and a hydrophobic block) are typically difficult to be dispersed in aqueous solutions without using organic solvents. For example, using a 50:50 (v/v) mixture of tetrahydrofuran (THF) and water, Su *et al.* prepared polyplexes of a polystyrene-*block*-poly(*N*-methyl-4-vinylpyridinium iodine) (PS-*b*-P4VPQ) with the number-average molecular weights (M_n) of the PS and P4VPQ block of 19 600 and 12 000, respectively.[13] In such a mixed solvent, precipitates of the PS-*b*-P4VPQ/DNA multilamellae could be formed with a THF swollen PS bilayer of 21.3 nm thickness and a P4VPQ brush/DNA/water bilayer of 10.6 nm thickness. To avoid the need of using organic solvents, here, we have developed a method of dispersing this lamella-forming PS-*b*-P4VPQ (MW = 19 600/12 000) in aqueous solutions by adding lipid as a dispersing agent. The structure of the resulting aggregates formed by mixing PS-*b*-P4VPQ with 1,2-dipalmi-

Received: December 21, 2015
Revised: January 25, 2016
Published: January 27, 2016

 © 2016 American Chemical Society

DOI: 10.1021/acs.langmuir.5b04672
Langmuir 2016, 32, 1828−1835

Table 1. Parameters of the Multilamellar Structural Model Used in Simulating the SANS Profiles

			d_{62}-DPPC + PS-*b*-P4VPQ					d_{62}-DPPC + PS-*b*-P4VPQ + DNA + $CaCl_2$		
d_{62}-DPPC (mM)			10							
PS-*b*-P4VPQ (mM)			0		0.05	0.1	0.2	0.3	0.1	
DNA (μM)									7.62	
$CaCl_2$ (mM)									0	10	50
d_{62}-DPPC multilamellae	Scale ($\times 10^{-3}$)		2.50 ± 0.04	1.00 ± 0.04	4.38 ± 0.04	5.29 ± 0.20	5.12 ± 0.04	4.07 ± 0.15	4.70 ± 0.20	3.03 ± 0.20	3.21 ± 0.03
	Lamellar spacing, D (Å)		64.9 ± 0.2		64.9	64.9	64.9	64.9	65.6 ± 0.2	79.6 ± 0.1	81.5 ± 0.1
	Hydrophobic Layer Thickness (δ_T) (Å)		18.3 ± 0.4		18.3	18.3	18.3	18.3	18.3 ± 0.4	19.0 ± 0.3	19.2 ± 0.3
	Hydrophilic Layer Thickness (δ_H) (Å)		10.5 ± 0.9		10.5	10.5	10.5	10.5	10.5 ± 0.9	13.6 ± 0.7	13.9 ± 0.8
	NSLD ($\times 10^{-6}$ Å^{-2})	Hydrophobic Layer	7.44 ± 0.01		7.44	7.44	7.44	7.44	7.56 ± 0.01	7.56 ± 0.01	7.56 ± 0.01
		Hydrophilic Layer	2.85 ± 0.04		2.85	2.85	2.85	2.85	2.67 ± 0.04	2.20 ± 0.04	2.10 ± 0.04
		Solvent	6.36		6.36	6.36	6.36	6.36	6.36	6.36	6.36
	# of Lamellar plates		2.0 ± 1.0	20.0 ± 1.0	6.0 ± 1.0	5.0 ± 1.0	5.0 ± 1.0	4.0 ± 1.0	6.0 ± 1.0	12.0 ± 1.0	11.0 ± 1.0
	Caille parameter		0.01 ± 0.01		0.09 ± 0.01	0.43 ± 0.01	0.54 ± 0.03	0.73 ± 0.03	0.37 ± 0.02	0.07 ± 0.01	0.11 ± 0.01
d_{62}-DPPC/PS-*b*-P4VPQ multilamellae	Scale ($\times 10^{-3}$)				0.96 ± 0.03	4.79 ± 0.01	8.47 ± 0.03	21.1 ± 0.5	4.70 ± 0.1	2.29 ± 0.2	3.47 ± 0.02
	Lamellar spacing, D (Å)				174.0 ± 0.5	174.0	174.0	174.0	203.1 ± 0.5	204.9 ± 0.6	214.6 ± 0.6
	Hydrophobic Layer Thickness (δ_T) (Å)				27.1 ± 0.1	27.1	27.1	27.1	27.0 ± 0.1	27.0	27.0
	Hydrophilic Layer Thickness (δ_H) (Å)				60.0 ± 1.1	60.0	60.0	60.0	61.0 ± 1.1	76.9 ± 1.7	77.0 ± 0.8
	NSLD ($\times 10^{-6}$ Å^{-2})	Hydrophobic Layer			3.86 ± 0.05	3.86	3.86	3.86	2.36 ± 0.05	2.36	2.36
		Hydrophilic Layer			5.60 ± 0.02	5.60	5.60	5.60	5.34 ± 0.02	5.33 ± 0.02	5.27 ± 0.03
		Solvent			6.36	6.36	6.36	6.36	6.36	6.36	6.36
	# of Lamellar plates				9.0 ± 1.0	8.0 ± 1.0	8.0 ± 1.0	8.0 ± 1.0	9.0 ± 1.0	6.0 ± 1.0	6.0 ± 1.0
	Caille parameter				1.94 ± 0.09	1.28 ± 0.01	1.55 ± 0.13	2.00 ± 0.08	0.82 ± 0.01	0.61 ± 0.01	0.74 ± 0.02

toyl-d_{62}-*sn*-glycero-3-phosphocholine (d_{62}-DPPC) in aqueous solutions and the multilamellae formed with DNA were investigated by small-angle neutron scattering (SANS). Using d_{62}-DPPC in D_2O reduces the scattering from the lipids and enhances the scattering contribution from the diblock copolymer domains. The effect of divalent ions on the cationic brush–DNA interaction was also investigated by adding calcium ions in the solution.

EXPERIMENTAL SECTION

Materials and Sample Preparation. The sodium salt of linear DNA of type XIV from herring testes was purchased from Sigma and used without further purification. The molecular weight of the DNA as determined by gel electrophoresis is between 400 and 1000 base pairs (a base pair has an average molecular weight of 649 g/mol), with an average around 700 base pairs.[14] Amphiphilic cationic diblock copolymer PS-*b*-P4VPQ was purchased from Polymer Source, Inc. The number-averaged molecular weights of the PS and P4VPQ blocks were 19 600 and 12 000 g/mol, respectively (corresponding to the degree of polymerization of 188 and 48). This PS-*b*-P4VPQ can form a stable monolayer at the air–water interface.[10] The polydispersity index M_w/M_n of the PS-*b*-P4VPQ is 1.08. Calcium chloride (95%) and D_2O (99.9%) were purchased from Sigma. d_{62}-DPPC was obtained from Cambridge Isotope, Inc., and its hydrophobic chain melting temperature is 42 °C. PS-*b*-P4VPQ and d_{62}-DPPC were first dissolved in chloroform and subsequently dried in vacuum to remove the solvent. D_2O, combined with sonication, was used to dissolve the dried mixture. The neutron scattering length density of the deuterated tails of d_{62}-DPPC and D_2O are equal to 7.74×10^{-6} and 6.36×10^{-6} Å^{-2}, respectively. Thus, in a D_2O solution, the scattering will therefore be mostly from the PS-*b*-P4VPQ in a mixture of d_{62}-DPPC/PS-*b*-P4VPQ. The neutron scattering length density of P4VPQ and PS blocks are 1.27×10^{-6} and 1.38×10^{-6} Å^{-2}, respectively.[10] The concentration of d_{62}-DPPC was kept at 10 mM, which means that all of the samples are fully hydrated, while the concentration of the PS-*b*-P4VPQ was increased from 0 to 0.05, 0.1, 0.2, and 0.3 mM.

SANS Measurements. SANS measurements were conducted on the QUOKKA instrument at the OPAL research reactor at ANSTO, Australia.[15] The SANS spectrometer provides high neutron intensity and a wide Q range using a 1 m^2 multiwire gas detector with the

DOI: 10.1021/acs.langmuir.5b04672
Langmuir 2016, 32, 1828–1835

capability to offset the detector to cover a wider Q range at a given sample–detector distance. The neutron wavelength was set by a velocity selector with λ = 4.94 Å and a wavelength spread of 6.7%. For each sample, the SANS data were collected at two detector positions, 2 m (with collimation length of 4 m) and 12 m (with collimation length of 12 m), to cover a continuous Q range from about 0.006 to 0.45 Å^{-1}. Here, Q is the scattering vector, defined as $Q = (4\pi/\lambda)\sin(\theta/2)$, where θ is the scattering angle between the scattered neutrons and the incident neutrons. The neutron source aperture size was 50 mm, and the sample aperture sizes were 5 and 7.5 mm for the detector positions of 2 and 12 m, respectively. The samples, contained in Hellma cuvettes, were kept at 25 °C during the SANS measurements using a thermostatically controlled circulation bath.

SANS Data Analysis. A multilamellar structural model was used for quantitatively analyzing the SANS profiles for both the d_{62}-DPPC and the d_{62}-DPPC/PS-*b*-P4VPQ multilamellae.[16] Data analysis was carried out using the National Institute of Standards and Technology (NIST) Center for Neutron Research (NCNR) SANS data analysis macros written for Igor Pro software.[17] The bilayer structure is divided into hydrophobic and hydrophilic layers. The SANS intensity, $I(Q)$, is proportional to the product of the bilayer form factor, $P(Q)$, and the interbilayer structure factor (lamellar structure factor), $S(Q)$, as given in the following:[16]

$$I(Q) = c\frac{2\pi P(Q)S(Q)}{dQ^2} \tag{1}$$

where c is the scale factor and d is the repeat spacing. The form factor $P(Q)$ is given by

$$P(Q) = \frac{4}{Q^2}\{\Delta\rho_H[\sin[Q(\delta_H + \delta_T)] - \sin(Q\delta_T)] + \Delta\rho_T \sin(Q\delta_T)\}^2 \tag{2}$$

where δ_H is the headgroup thickness (hydrophilic layer thickness), δ_T is the tail length (hydrophobic layer thickness), $\Delta\rho_H$ is the difference between the headgroup NSLD and the solvent NSLD, and $\Delta\rho_T$ is the difference between the tail NSLD and the solvent NSLD, where NSLD is the coherent neutron scattering length density.

The structure factor $S(Q)$ is given by

$$S(Q) = 1 + 2\sum_{1}^{N-1}\left(1 - \frac{n}{N}\right)\cos\left(\frac{Qdn}{1 + 2\Delta Q^2d^2\alpha(n)}\right) \exp\left(-\frac{2Q^2d^2\alpha(n) + \Delta Q^2d^2n^2}{2(1 + 2\Delta Q^2d^2\alpha(n))}\right)\frac{1}{\sqrt{1 + 2\Delta Q^2d^2\alpha(n)}} \tag{3}$$

where

$$\alpha(n) = \frac{\eta_{cp}}{4\pi^2}[\ln(\pi n) + \gamma_E] \tag{4}$$

where γ_E is Euler's constant (γ_E = 0.577 215 664 9), η_{cp} is the Caillé parameter, ΔQ is the instrumental resolution, and N is the number of lamellar plates.

Both the layer thickness and the neutron scattering length density of the multilamellae can be determined from analyzing the SANS profiles. The lamellar structure factor describes the interbilayer correlation, which depends upon the lamellar repeat distance, number of bilayer stacks, and membrane flexibility (Caillé parameter, η_{cp}).[16,18,19] The parameters of the multilamellar structural model used in simulating the SANS profiles are listed in Table 1.

RESULTS AND DISCUSSION

Figure 1 shows the measured SANS profiles from solutions of mixed d_{62}-DPPC/PS-*b*-P4VPQ multilamellae at different PS-*b*-P4VPQ to d_{62}-DPPC ratios in D_2O at 25 °C. For the pure d_{62}-DPPC sample, i.e., in the absence of the diblock copolymer, the double-tail zwitterionic d_{62}-DPPC forms multilamellae in

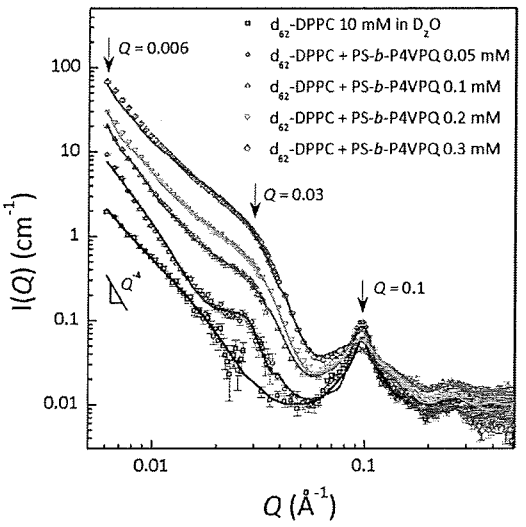

Figure 1. SANS profiles from the mixture of d_{62}-DPPC and PS-*b*-P4VPQ in D_2O at 25 °C. The concentration of d_{62}-DPPC was kept at 10 mM for all samples.

aqueous solutions. Although the deuterated tails of d_{62}-DPPC and D_2O have similar neutron scattering length densities, the head groups of the d_{62}-DPPC, with a neutron scattering length density of 1.73 × 10^{-6} Å^{-2} and a volume of 348 Å^3, still contribute some scattering. As a result, the scattering profile still exhibits a diffraction peak at Q = 0.097 Å^{-1}, which corresponds to the lamellar d spacing of 6.5 nm for the d_{62}-DPPC lipid bilayers. The SANS profile of the pure d_{62}-DPPC multilamellae was fitted with two multilamellar groups with different bilayer stacking numbers to obtain the best fit. As shown in Figure 1, the low-Q region is characterized by a power law dependence of ca. Q^{-4} that signifies interfacial scattering from large objects, in this case, the multilamellae. With the addition of PS-*b*-P4VPQ, the location of the d_{62}-DPPC multilamellar diffraction peak remains unchanged but its peak intensity decreases with increasing the PS-*b*-P4VPQ concentration. Because the peak width is essentially about the same, it indicates a reduction in the number of "pure" d_{62}-DPPC multilamellae in solution as a result of the addition of PS-*b*-P4VPQ (see Figure S1 of the Supporting Information). Simultaneously, broad correlation peaks appear upon the addition of PS-*b*-P4VPQ. This broad correlation peak can be attributed to the not well ordered d_{62}-DPPC/PS-*b*-P4VPQ multilamellae, as indicated by the relatively large Caillé parameter obtained by fitting. The peak position of the broad correlation peak may not be easily identified by directly looking at the scattering profiles because it sits on the big Q^{-4} slope. The apparent peak position is around Q = 0.030–0.036 Å^{-1}, which is not too far from the Q peak calculated from the $2\pi/d$ = 0.036 Å^{-1} with a multilamellar d spacing of 174 Å, as determined from the model fitting. The apparent peak position of the correlation peak can also be affected by the high fluctuation of the multilamellae as a result of the higher Caillé parameter obtained from fitting the SANS profiles.

As more PS-*b*-P4VPQ is added, both the intensity of this broad correlation peak and the scattering intensity in the low-Q region increase. The decrease of the d_{62}-DPPC diffraction peak intensity at Q = 0.097 Å^{-1}, the increase of the low-Q scattering intensity, and the increase in the d_{62}-DPPC/PS-*b*-P4VPQ

DOI: 10.1021/acs.langmuir.5b04672
Langmuir 2016, 32, 1828–1835

correlation peak intensity all indicate that the d_{62}-DPPC multilamellae are gradually depleted to form more d_{62}-DPPC/PS-*b*-P4VPQ multilamellae as more PS-*b*-P4VPQ is added. It is clear that the lipids act as dispersing agents to disperse the lamella-forming PS-*b*-P4VPQ in aqueous solutions. Figure S2 of the Supporting Information shows that the scattering intensity at $Q = 0.0061$ Å^{-1} increases roughly linearly as a function of the added amounts of PS-*b*-P4VPQ. It indicates that more d_{62}-DPPC/PS-*b*-P4VPQ multilamellae are formed as more PS-*b*-P4VPQ is added.

A monolayer mixture of lipid with a diblock copolymer, such as DPPC with PS-*b*-P4VPQ (MW = 19 600/12 000), could exhibit microscopic phase separation with lipid domains mixed with diblock copolymer domains.[20] Similarly, it was also found that the morphology of the bilayer of giant unilamellar vesicles composed of lamella-forming graft copolymer polydimethylsiloxane-*co*-polyethylene oxide (PDMS-*co*-PEO) and DPPC exhibits patch- and stripe-shaped domains.[21] These studies show that lamella-forming diblock copolymers could form stable domains in coexistence with DPPC domains.[21,22] In this way, the PS-*b*-P4VPQ could be dispersed into small domains that are intercalated between the d_{62}-DPPC domains. Without the help of d_{62}-DPPC, the lamella-forming PS-*b*-P4VPQ could not be dispersed in aqueous solution and could not be used to form multilamellae with DNA. Because PS-*b*-P4VPQ used here is a lamella-forming diblock copolymer, the measured *d* spacing of 17.4 nm would be roughly equal to 2 times the sum of the PS layer thickness and the P4VPQ brush layer thickness. The neutron reflectometry study on the PS-*b*-P4VPQ monolayer at the air–water interface showed that the PS layer has a thickness of about 3.2 nm and the P4VPQ forms a dense brush layer of about 5.1 nm thickness and a loose brush layer of about 4.2 nm thickness.[10] Although, in the bulk solution with a bilayer structure, the layer thicknesses could be slightly different from that in the monolayer at the air–water interface, we can still use the monolayer data to give a crude estimate of the bilayer thickness. If one assumes that the PS-*b*-P4VPQ bilayers are in close contact, a repeat distance of 2(PS layer + P4VPQ dense brush layer) = 2(3.2 + 5.1 nm) = 16.6 nm would be obtained. Here, only the dense brush layer thickness is taken into account. This value is quite close to the measured *d* spacing of 17.4 nm for the d_{62}-DPPC/PS-*b*-P4VPQ multilamellae. Loose brushes extending out from the dense brush layer could also affect the *d* spacing.

The SANS profiles were analyzed using the multilamellar model described in the data analysis section, and the results are summarized in Table 1. The SANS profiles were all well-fitted with the multilamellar model, as shown in Figure 1. The thicknesses of the hydrophobic layer and the hydrophilic layer of the d_{62}-DPPC/PS-*b*-P4VPQ multilamellar bilayer were found to be 2.7 and 6.0 nm, respectively. These values are comparable to the 3.2 nm hydrophobic PS layer and the 5.1 nm dense P4VPQ brush layer revealed from our previous neutron reflectometry study.[10] The hydrophobic layer thickness in the multilamellae is slightly smaller than that in the monolayer, which could be due to mixing with the d_{62}-DPPC domains to form a mixed bilayer system. The obtained hydrophilic layer thickness of 6.0 nm is slightly larger than the dense brush layer thickness of 5.1 nm, which indicates that the loose brushes contribute to the total brush layer thickness in the bilayer form. In such a multilamellar system, the loose brushes must be squeezed and could be mutually penetrating. According to the model fitting, the neutron scattering length density of the hydrophobic layer of the multilamellae is found to be 3.86×10^{-6} Å^{-2}, which is higher than 1.38×10^{-6} Å^{-2} for the pure PS layer. This higher neutron scattering length density should be due to the contribution from the deuterated hydrocarbon tails of d_{62}-DPPC incorporated in the multilamellae. The volume fraction of the deuterated tails of the d_{62}-DPPC in the hydrophobic layer of the d_{62}-DPPC/PS-*b*-P4VPQ multilamellae can be deduced to be 0.39 for the 0.1 mM PS-*b*-P4VPQ case. Using the estimated volume of the d_{62}-DPPC tails of 862 Å^3 and the volume of one PS block of 31 900 Å^3, it is possible to estimate the amounts of the d_{62}-DPPC in the d_{62}-DPPC/PS-*b*-P4VPQ multilamellae to be about 2.4 mM for the 0.1 mM PS-*b*-P4VPQ case. As for the neutron scattering length density of the hydrophilic layer of the multilamellae, it is found to be 5.60×10^{-6} Å^{-2}; this value is very close to 5.66×10^{-6} Å^{-2} found for the neutron scattering length density of the dense brush layer in the PS-*b*-P4VPQ monolayer at the air–D_2O interface.[10] In the PS-*b*-P4VPQ monolayer case, there is about 86% D_2O by volume in the dense brush layer, which results in a high value of the averaged neutron scattering length density of the hydrophilic layer.[10] The volume fraction of D_2O in the hydrophilic layer of the d_{62}-DPPC/PS-*b*-P4VPQ multilamellae can be estimated in similar ways.[10]

The cationic brush of PS-*b*-P4VPQ interacts strongly with the DNA, and DNA could be adsorbed in the brush layer of the multilamellae. Figure 2 shows the changes in the SANS profile

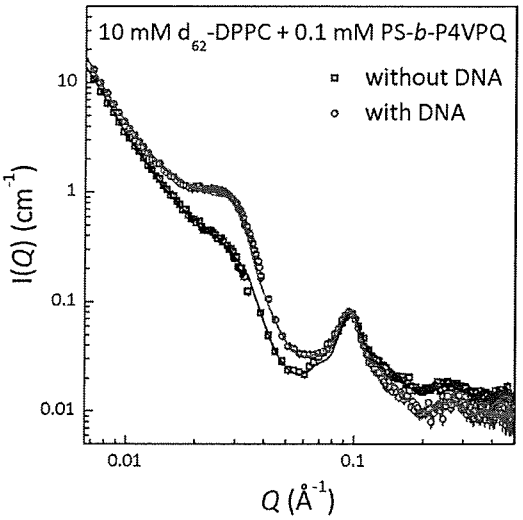

Figure 2. SANS profiles from the mixture of 10 mM d_{62}-DPPC and 0.1 mM PS-*b*-P4VPQ without and with 7.26 μM DNA (average of 700 bp) at 25 °C.

of the 10 mM d_{62}-DPPC/0.1 mM PS-*b*-P4VPQ multilamellae system when 7.26 μM DNA is added. As shown in Figure 2, the enhancement of the correlation peak at around $Q \sim 0.031$ Å^{-1} is notable when DNA is added. The d_{62}-DPPC multilamellar diffraction peak at around $Q \sim 0.096$ Å^{-1} is not changed much as a result of the addition of DNA. This is due to zwitterionic d_{62}-DPPC multilamellae interacting very weakly with DNA without the presence of multivalent cations.[23,24] The d_{62}-DPPC/PS-*b*-P4VPQ multilamellae interact strongly with DNA. The addition of DNA enhances the broad correlation peak intensity and slightly moves the correlation peak toward a lower Q region, which corresponds to a slightly larger *d* spacing of

DOI: 10.1021/acs.langmuir.5b04672
Langmuir 2016, 32, 1828–1835

about 20.3 nm, as determined from the model fitting. The increase in d spacing signifies the adsorption of DNA in the cationic brush layer of the d_{62}-DPPC/PS-*b*-P4VPQ multilamellae. The brush layer is swollen as a result of the adsorption of DNA. As listed in Table 1, the neutron scattering length density of the hydrophilic layer for the d_{62}-DPPC/PS-*b*-P4VPQ/DNA multilamellae is found to decrease slightly from 5.60×10^{-6} Å^{-2} for the case without DNA to 5.34×10^{-6} Å^{-2}. The decrease in neutron scattering length density is due to the adsorption of DNA, which occupied the space originally occupied by D_2O, and also DNA has a lower neutron scattering length density (around 4.1×10^{-6} Å^{-2}) than D_2O (6.36×10^{-6} Å^{-2}). The volume fraction of adsorbed DNA in the hydrophilic layer can be estimated from the drop of the neutron scattering length density, and it is found to be around 11.5%. This decrease in neutron scattering length density serves to enhance the scattering contrast and therefore intensity. The decrease in the neutron scattering length density of the hydrophilic layer of adsorbed DNA of the d_{62}-DPPC/PS-*b*-P4VPQ/DNA multilamellae is not as great as that as for DNA adsorption by the PS-*b*-P4VPQ monolayer at the air–water interface, suggesting that the amount of adsorbed DNA by the multilamellae is less than that for the PS-*b*-P4VPQ monolayer.[10]

Moreover, there is an unexpected slight neutron scattering length density drop, from 3.86×10^{-6} to 2.36×10^{-6} Å^{-2}, of the hydrophobic layer in the d_{62}-DPPC/PS-*b*-P4VPQ/DNA multilamellae. This implies that the composition of the hydrophobic layer has somewhat changed. The volume fraction of the PS block, χ_{PS}, in the hydrophobic layer of the multilamellae can be estimated from the neutron scattering length density ρ_b of the hydrophobic layer of the d_{62}-DPPC/PS-*b*-P4VPQ multilamellae phase, via $\rho_b = \rho_{PS}\chi_{PS} + \rho_{d\text{-tail}}(1 - \chi_{PS})$, where ρ_{PS} is the neutron scattering length density of the PS blocks and $\rho_{d\text{-tail}}$ is the neutron scattering length density of the deuterated hydrophobic tails of d_{62}-DPPC. According to this calculation, χ_{PS} is found to change from 0.61 to 0.85 before and after adding DNA, respectively. This means that PS-*b*-P4VPQ domains can be stabilized by the adsorption of DNA in their cationic brushes and less d_{62}-DPPC is needed in dispersing the PS-*b*-P4VPQ in the presence of DNA. As less d_{62}-DPPC is present within the d_{62}-DPPC/PS-*b*-P4VPQ multilamellae, the average neutron scattering length density of the hydrophobic layer would decrease. The stabilization effect could be due to the fact that the adsorption of DNA might induce the PS-*b*-P4VPQ domains to fuse into larger domains and reduce the number of d_{62}-DPPC domains needed to disperse the PS-*b*-P4VPQ domains. Indeed, a previous study on the cationic bicelle–DNA multilamellar system also found that the adsorption of DNA could cause the bicelles to fuse into larger bicelles when forming multilamellae with DNA.[9]

The total thickness of the hydrophilic region between the hydrophobic layers increases from 12.0 nm ($17.4 - 2 \times 2.7$) to 14.9 nm ($20.3 - 2 \times 2.7$) as a result of the adsorption of DNA. The other study on the PS-*b*-P4VPQ/DNA multilamellae by dissolving in a 50:50 (v/v) THF/water mixture revealed that the total hydrophilic layer thickness is about 15.3 nm when rehydrated in water.[13] The thicknesses of the hydrophilic region for these two systems, dispersed with the help of lipid and THF/water, are quite close. However, the thickness of the hydrophobic region for the THF/water system is swollen to 15.3 nm as a result of the presence of THF in the hydrophobic layer.[13] For the lipid dispersed system in aqueous solution, the thickness of the hydrophobic region is only $2 \times 2.7 = 5.4$ nm.

The bending rigidity of the d_{62}-DPPC/PS-*b*-P4VPQ/DNA multilamellae can also be examined by checking the Caillé parameter η_{cp} determined from the model fitting. According to the definition, the Caillé parameter η_{cp} is a measure of the bilayer fluctuations and inversely proportional to the square root of the bilayer bending rigidity. On the other words, η_{cp} becomes larger when the membrane has a lower bending rigidity. For cases without DNA and calcium ions, the d_{62}-DPPC/PS-*b*-P4VPQ multilamellae have a relatively large η_{cp} of around 1.3–2.0, which indicates that the d_{62}-DPPC/PS-*b*-P4VPQ multilamellae have a lower bending rigidity than the lipid multilamellae. The presence of PS-*b*-P4VPQ significantly alters the lamellar mechanical property by not only increasing its fluctuations and but also decreasing its rigidity. As for the cases with the addition of DNA, η_{cp} of the d_{62}-DPPC/PS-*b*-P4VPQ/DNA multilamellae is reduced back to around 0.6–0.8, which indicates that the presence of DNA could stabilize the ordering of the multilamellae by reducing the fluctuations and increasing its rigidity.

Divalent cations can play important roles on the formation of the lipid–DNA mixture for gene delivery applications.[25–27] In the case of the cationic lipid–DNA mixture, calcium, the most common divalent cations in an organism, can induce DNA condensation and regulate the columnar spacing of DNA arrays in a cationic lipid–DNA mixture.[28] For anionic lipid–DNA multilamellae, divalent cations act as glue between the negatively charged lipid bilayer surface and DNA and could further induce structural transitions at high calcium concentrations.[26,29] As mentioned earlier, for the zwitterionic lipid bilayer system, such as DPPC or DOPC, the interaction between the lipid bilayer and DNA is rather weak and could not form stable lipid–DNA multilamellae. However, the addition of calcium ions can turn zwitterionic lipids to become cationic by incorporating the calcium ions in the headgroup, and the complexation with DNA becomes possible.[25,27,30–32] This is apparent as shown in Figure 3, which shows the effect of adding

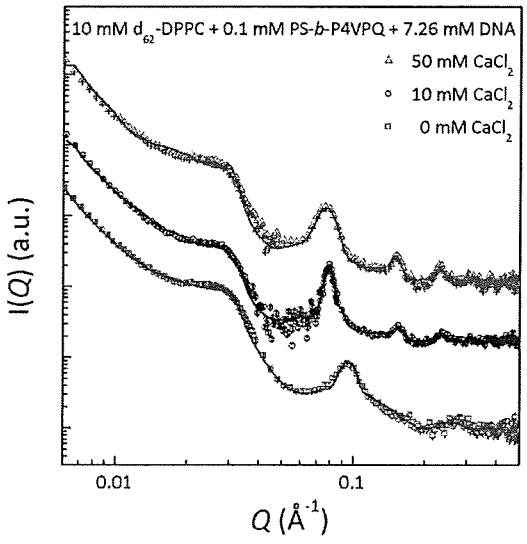

Figure 3. SANS profiles from the mixture of d_{62}-DPPC and PS-*b*-P4VPQ in the presence of 7.26 μM DNA (average of 700 bp) without and with 10 and 50 mM $CaCl_2$ at 25 °C.

DOI: 10.1021/acs.langmuir.5b04672
Langmuir 2016, 32, 1828–1835

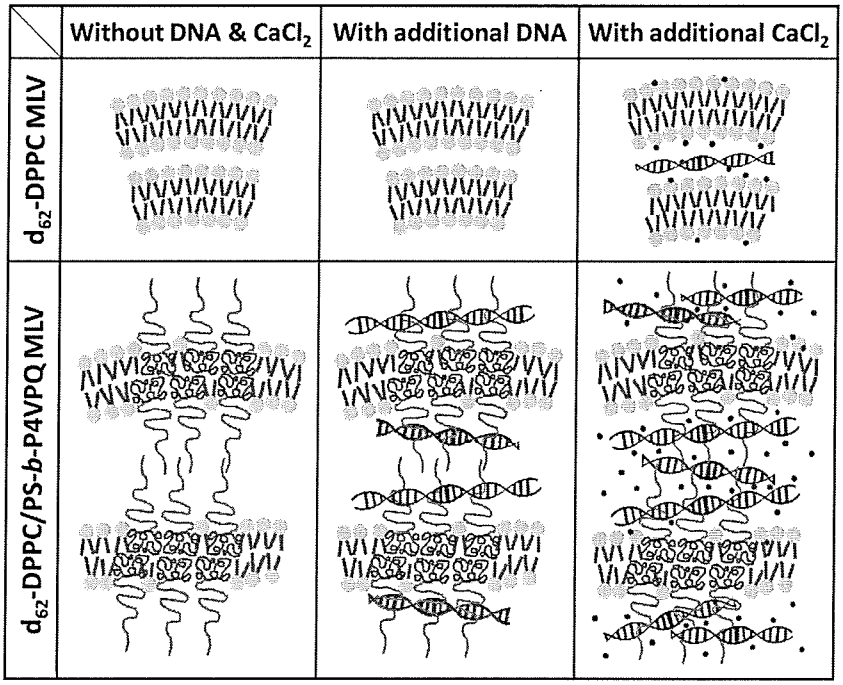

Figure 4. Schematic of the mixture of d_{62}-DPPC and PS-*b*-P4VPQ without and with DNA and $CaCl_2$. The calcium ions are represented as red dots. The system consists of pure d_{62}-DPPC multilamellae and d_{62}-DPPC/PS-*b*-P4VPQ multilamellae. The DNA molecules are represented as helices in blue color.

10 and 50 mM calcium ions on the adsorption of DNA by the 10 mM d_{62}-DPPC/0.1 mM PS-*b*-P4VPQ mixture. Upon the addition of 10 and 50 mM $CaCl_2$, the d_{62}-DPPC multilamellar peak position moves from 0.097 to 0.079 and 0.077 $Å^{-1}$, respectively, and the *d* spacing increases from 6.5 to 8.0 and 8.2 nm, respectively, for 0, 10, and 50 mM $CaCl_2$. The increase of the *d* spacing is due to the adsorption of DNA molecules that are encapsulated between the d_{62}-DPPC bilayers.[30] The higher order lamellar diffraction peaks of the d_{62}-DPPC/$CaCl_2$/DNA multilamelae are also clearly visible, indicating the formation of highly ordered d_{62}-DPPC/$CaCl_2$/DNA multilamellae in the presence of $CaCl_2$. The increase of the $CaCl_2$ concentration from 10 to 50 mM slightly broadens the d_{62}-DPPC/$CaCl_2$/DNA multilamellar peak and also induces a very slight further increase of the *d* spacing.

As for the effect of adding $CaCl_2$ on the d_{62}-DPPC/PS-*b*-P4VPQ/DNA multilamellae, the position of the correlation peak is largely unaffected. The layer thickness and the neutron scattering length density of the hydrophobic layer of the d_{62}-DPPC/PS-*b*-P4VPQ/DNA multilamellae are not affected by the addition of $CaCl_2$. However, it is found that the addition of $CaCl_2$ induces swelling of the hydrophilic layer of the d_{62}-DPPC/PS-*b*-P4VPQ/DNA multilamellae by 1.6 nm. The swelling can be attributed to the increase in DNA adsorption in the brush layer as a result of the addition of $CaCl_2$. If the swelling of the hydrophilic layer is purely by the brushes only, i.e., without incorporating more DNA, the average neutron scattering length density of the swollen hydrophilic layer would increase as a result of the increase of D_2O molecules in the hydrophilic layer. In fact, the neutron scattering length density of the swollen hydrophilic layer does not increase but decreases slightly. This is an indication that the swelling is accompanied by an increase in DNA adsorption. To maintain the same neutron scattering length density, approximately 55% of the swollen volume should be occupied by D_2O and the other 45% of the swollen volume should be occupied by DNA, viz., $(6.36 \times 10^{-6}) \times 0.55 + (4.1 \times 10^{-6}) \times 0.45 = 5.34 \times 10^{-6}$ $Å^{-2}$. The increase of $CaCl_2$ from 10 to 50 mM further reduces the neutron scattering length density of the hydrophilic layer from 5.33×10^{-6} to 5.25×10^{-6} $Å^{-2}$, which indicates a slight increase of DNA adsorption by the cationic brushes. This enhancement in DNA adsorption is similar to what happens in the PS-*b*-P4VPQ diblock copolymer monolayer at the air–water interface as a result of the addition of $CaCl_2$.[10] The schematics of the d_{62}-DPPC multilamellae and d_{62}-DPPC/PS-*b*-P4VPQ multilamellae without and with DNA and $CaCl_2$ are shown in Figure 4.

■ CONCLUSION

It is demonstrated in this study that the lamella-forming PS-*b*-P4VPQ can be dispersed in an aqueous solution by mixing with lipids. The mixed d_{62}-DPPC/PS-*b*-P4VPQ exhibits a multilamellar bilayer structure, which has a lamellar *d* spacing of 17.4 nm with a 2.7 nm hydrophobic layer and a 6.0 nm hydrophilic layer. The extra d_{62}-DPPC forms pure lipid multilamellae in coexistence with the d_{62}-DPPC/PS-*b*-P4VPQ multilamellae. It is important to know whether the d_{62}-DPPC/PS-*b*-P4VPQ multilamellae can be used to adsorb DNA or not. SANS analysis shows that DNA can indeed be adsorbed by the cationic brushes in the hydrophilic layer of the d_{62}-DPPC/PS-*b*-P4VPQ multilamellae, while the pure d_{62}-DPPC multilamellae have a very weak interaction with DNA. DNA adsorption can be enhanced by the addition of divalent cations. DNA also plays a role as a stabilizer in d_{62}-DPPC/PS-*b*-P4VPQ multilamellae to form larger domains of d_{62}-DPPC/PS-*b*-P4VPQ/DNA lamellar structure by reducing the amounts of

DOI: 10.1021/acs.langmuir.5b04672
Langmuir 2016, 32, 1828–1835

lipid required to disperse the PS-*b*-P4VPQ. In the presence of calcium ions, further DNA condensation is evident for the d_{62}-DPPC/PS-*b*-P4VPQ multilamellar phase and the enhanced DNA adsorption induces a slight swelling of the hydrophilic layer of the d_{62}-DPPC/PS-*b*-P4VPQ multilamellae. The enhanced DNA adsorption by the cationic brushes is similar to that found in the study of DNA adsorption by the PS-*b*-P4VPQ diblock copolymer monolayer at the air–water interface when adding $CaCl_2$. These findings should be helpful for developing novel DNA encapsulation systems for gene delivery and for DNA immobilization in DNA microarrays.

■ ASSOCIATED CONTENT

Supporting Information

The Supporting Information is available free of charge on the ACS Publications website at DOI: 10.1021/acs.langmuir.5b04672.

d_{62}-DPPC multilamellar peaks around $Q \sim 0.1$ Å^{-1} in coexistence with the d_{62}-DPPC/PS–P4VPQ multilamellae plotted by carefully subtracting the contribution from the d_{62}-DPPC/PS–P4VPQ multilamellae (Figure S1) and SANS intensities at $Q = 0.0061$ Å^{-1} from the mixture of d_{62}-DPPC and PS-*b*-P4VPQ in D_2O as a function of the PS-*b*-P4VPQ concentration (Figure S2) (PDF)

■ AUTHOR INFORMATION

Corresponding Author

*Telephone: +886-3-5742671. Fax: 886-3-5728445. E-mail: tllin@mx.nthu.edu.tw.

Notes

The authors declare no competing financial interest.

■ ACKNOWLEDGMENTS

The authors thank the Bragg Institute, ANSTO, Australia, for providing the Quokka SANS beam time and the assistance during the experiment. The travel funding for the SANS experiment was supported by the Ministry of Science and Technology, Project MOST 103-2739-M-213-001-MY3, managed by the Neutron User Program, NSRRC, Taiwan, Republic of China. This research is supported by the National Science Council, Project NSC 99-2113-M-007-014-MY3, and the Ministry of Science and Technology, Taiwan, Republic of China, Project MOST 103-2113-M-007-014-MY2 (to Tsang-Lang Lin). This research is also partly supported by the Frontier Research Center on Fundamental and Applied Sciences of Matters of National Tsing Hua University, Project 102N2012E1.

■ REFERENCES

(1) Huang, S.-L. Liposomes in ultrasonic drug and gene delivery. *Adv. Drug Delivery Rev.* **2008**, *60*, 1167–1176.

(2) Puri, A.; Loomis, K.; Smith, B.; Lee, J.-H.; Yavlovich, A.; Heldman, E.; Blumenthal, R. Lipid-Based Nanoparticles as Pharmaceutical Drug Carriers: From Concepts to Clinic. *Crit. Rev. Ther. Drug Carrier Syst.* **2009**, *26*, 523–580.

(3) Schaefer, J.; Hoebel, S.; Bakowsky, U.; Aigner, A. Liposome-polyethylenimine complexes for enhanced DNA and siRNA delivery. *Biomaterials* **2010**, *31*, 6892–6900.

(4) Tros de Ilarduya, C.; Sun, Y.; Duezguenes, N. Gene delivery by lipoplexes and polyplexes. *Eur. J. Pharm. Sci.* **2010**, *40*, 159–170.

(5) Tseng, Y.-C.; Mozumdar, S.; Huang, L. Lipid-based systemic delivery of siRNA. *Adv. Drug Delivery Rev.* **2009**, *61*, 721–731.

(6) Natali, F.; Castellano, C.; Pozzi, D.; Castellano, A. C. Dynamic Properties of an Oriented Lipid/DNA Complex Studied by Neutron Scattering. *Biophys. J.* **2005**, *88*, 1081–1090.

(7) Gerelli, Y.; Di Bari, M. T.; Barbieri, S.; Sonvico, F.; Colombo, P.; Natali, F.; Deriu, A. Flexibility and drug release features of lipid/saccharide nanoparticles. *Soft Matter* **2010**, *6*, 685–691.

(8) Wu, J.-C.; Lin, T.-L.; Jeng, U. S.; Lee, H.-Y.; Gutberlet, T. Neutron and X-ray reflectivity studies on DNA adsorption on mixed DPPC/DC-cholesterol monolayers. *Phys. B* **2006**, *385–386*, 841–844.

(9) Yang, P.-W.; Lin, T.-L.; Lin, T.-Y.; Yang, C.-H.; Hu, Y.; Jeng, U. S. Packing DNA with disc-shaped bicelles. *Soft Matter* **2013**, *9*, 11542–11548.

(10) Yang, P.-W.; Lin, T.-L.; Liu, I. T.; Hu, Y.; James, M. In situ neutron reflectivity studies of the adsorption of DNA by charged diblock copolymer monolayers at the air-water interface. *Soft Matter* **2012**, *8*, 7161–7168.

(11) Korobko, A. V.; Jesse, W.; van der Maarel, J. R. C. Encapsulation of DNA by cationic diblock copolymer vesicles. *Langmuir* **2005**, *21*, 34–42.

(12) Kakizawa, Y.; Kataoka, K. Block copolymer micelles for delivery of gene and related compounds. *Adv. Drug Delivery Rev.* **2002**, *54*, 203–222.

(13) Su, C. J.; Yeh, S. W.; Lai, W. C.; Chen, H. L.; Rahman, M. H.; Wu, R. J.; Lin, H. K.; Liu, W. L. Condensed multilamellar structure of a complex of DNA with an amphiphilic block copolymer. *Soft Matter* **2008**, *4*, 1306–1312.

(14) Garcia-Diaz, M.; Dominguez, O.; Lopez-Fernandez, L. A.; de Lera, L. T.; Saniger, M. L.; Ruiz, J. F.; Parraga, M.; Garcia-Ortiz, M. J.; Kirchhoff, T.; del Mazo, J.; Bernad, A.; Blanco, L. DNA polymerase lambda (Pol lambda), a novel eukaryotic DNA polymerase with a potential role in meiosis. *J. Mol. Biol.* **2000**, *301*, 851–867.

(15) Gilbert, E. P.; Schulz, J. C.; Noakes, T. J. 'Quokka'—The small-angle neutron scattering instrument at OPAL. *Phys. B* **2006**, *385–386*, 1180–1182.

(16) Nallet, F.; Laversanne, R.; Roux, D. Modeling X-ray or Neutron-Scattering Spectra of Lytropic Lamellar Phase-Interplay between Form and Structure Factors. *J. Phys. II* **1993**, *3*, 487–502.

(17) Kline, S. R. Reduction and analysis of SANS and USANS data using IGOR Pro. *J. Appl. Crystallogr.* **2006**, *39*, 895–900.

(18) Berghausen, J.; Zipfel, J.; Lindner, P.; Richtering, W. Influence of Water-Soluble Polymers on the Shear-Induced Structure Formation in Lyotropic Lamellar Phases. *J. Phys. Chem. B* **2001**, *105*, 11081–11088.

(19) Pabst, G.; Rappolt, M.; Amenitsch, H.; Laggner, P. Structural information from multilamellar liposomes at full hydration: Full Q-range fitting with high quality x-ray data. *Phys. Rev. E: Stat. Phys., Plasmas, Fluids, Relat. Interdiscip. Top.* **2000**, *62*, 4000–4009.

(20) Liu, I. T. Adsorption of DNA by Charged Diblockcopolymer and Lipid Monolayer at the Air–Water Interface by Langmuir–Blodgett Method and X-ray/Neutron Reflectivity. Master's Thesis, National Tsing Hua University, Hsinchu, Taiwan, Republic of China, July 2010.

(21) Chen, D.; Santore, M. M. Hybrid copolymer-phospholipid vesicles: Phase separation resembling mixed phospholipid lamellae, but with mechanical stability and control. *Soft Matter* **2015**, *11*, 2617–2626.

(22) Schulz, M.; Glatte, D.; Meister, A.; Scholtysek, P.; Kerth, A.; Blume, A.; Bacia, K.; Binder, W. H. Hybrid lipid/polymer giant unilamellar vesicles: Effects of incorporated biocompatible PIB-PEO block copolymers on vesicle properties. *Soft Matter* **2011**, *7*, 8100–8110.

(23) Ainalem, M.-L.; Kristen, N.; Edler, K. J.; Höök, F.; Sparr, E.; Nylander, T. DNA Binding to Zwitterionic Model Membranes. *Langmuir* **2010**, *26*, 4965–4976.

(24) Dabkowska, A. P.; Barlow, D. J.; Clifton, L. A.; Hughes, A. V.; Webster, J. R. P.; Green, R. J.; Quinn, P. J.; Lawrence, M. J. Calcium-mediated binding of DNA to 1,2-distearoyl-sn-glycero-3-phosphocholine-containing mixed lipid monolayers. *Soft Matter* **2014**, *10*, 1685–1695.

DOI: 10.1021/acs.langmuir.5b04672
Langmuir 2016, 32, 1828–1835

(25) McManus, J. J.; Rädler, J. O.; Dawson, K. A. Does Calcium Turn a Zwitterionic Lipid Cationic? *J. Phys. Chem. B* **2003**, *107*, 9869−9875.
(26) Yang, P.-W.; Lin, T.-L.; Hu, Y.; Jeng, U. S. Formation of divalent ion mediated anionic disc bicelle-DNA complexes. *Soft Matter* **2014**, *10*, 2313−2319.
(27) McManus, J. J.; Rädler, J. O.; Dawson, K. A. Observation of a Rectangular Columnar Phase in a DNA−Calcium−Zwitterionic Lipid Complex. *J. Am. Chem. Soc.* **2004**, *126*, 15966−15967.
(28) Gromelski, S.; Brezesinski, G. DNA Condensation and Interaction with Zwitterionic Phospholipids Mediated by Divalent Cations. *Langmuir* **2006**, *22*, 6293−6301.
(29) Liang, H. J.; Harries, D.; Wong, G. C. L. Polymorphism of DNA-anionic liposome complexes reveals hierarchy of ion-mediated interactions. *Proc. Natl. Acad. Sci. U. S. A.* **2005**, *102*, 11173−11178.
(30) McManus, J. J.; Rädler, J. O.; Dawson, K. A. Phase Behavior of DPPC in a DNA−Calcium−Zwitterionic Lipid Complex Studied by Small-Angle X-ray Scattering. *Langmuir* **2003**, *19*, 9630−9637.
(31) Uhríková, D.; Hanulová, M.; Funari, S. S.; Khusainova, R. S.; Šeršeň, F.; Balgavý, P. The structure of DNA−DOPC aggregates formed in presence of calcium and magnesium ions: A small-angle synchrotron X-ray diffraction study. *Biochim. Biophys. Acta, Biomembr.* **2005**, *1713*, 15−28.
(32) Mengistu, D. H.; Bohinc, K.; May, S. Binding of DNA to Zwitterionic Lipid Layers Mediated by Divalent Cations. *J. Phys. Chem. B* **2009**, *113*, 12277−12282.

DOI: 10.1021/acs.langmuir.5b04672
Langmuir 2016, 32, 1828−1835